LETTER

The influence of the optimal velocity deviation on the traffic evolution process under lane change in two-lane lattice model

To cite this article: Xiaoqin Li *et al* 2023 *EPL* **141** 33001

A Letters Journal Exploring the Frontiers of Physics

February 2023

EPL, **141** (2023) 33001
doi: 10.1209/0295-5075/acb2f3

www.epljournal.org

The influence of the optimal velocity deviation on the traffic evolution process under lane change in two-lane lattice model

Xiaoqin Li[1], Can Jin[2(a)] and Guanghan Peng[3(b)]

[1] *College of Mathematics and Physics Science, Hunan University of Arts and Science - Changde 415000, China*
[2] *Information and Modern Education Technology Center, Hunan University of Arts and Science - Changde 415000, China*
[3] *College of Physical Science and Technology, Guangxi Normal University - Guilin 541004, China*

received 10 August 2022; accepted in final form 13 January 2023
published online 25 January 2023

Abstract – In a real traffic environment, there is always a certain deviation between the real traffic information and the expected traffic information, which definitely has an important impact on traffic flow. Consequently, the optimal velocity deviation effect (OVDE) is taken into account to build a novel lattice model on two lanes. Moreover, the influence of OVDE on the linear stable condition is investigated, which shows that the OVDE plays a positive stable effect in two-lane traffic flow. Also, the OVDE can relieve more traffic congestion on two lanes via numerical simulations concerning the density and the hysteresis loop.

Introduction. – Recently, people have paid more and more attention to the traffic condition of urban roads. In order to simulate the evolution process of traffic, mathematical modeling is important to investigate traffic flow. Therefore, some researchers have proposed their own traffic flow models [1–11]. Also, Zeng *et al.* [12,13] and Ma *et al.* [14,15] executed traffic modeling based on traffic predicting. Moreover, Nagatani [16,17] provided the lattice model on single lane which has attracted the attention of some scholars [18–46]. To investigate lane changing behaviors, Nagatani [47] further built a lattice model of two-lane traffic with lane changing rate. Also, different traffic factors [48–59] have been studied to develop two-lane lattice models. In real traffic, the optimal velocity reflects the driver's expectation of traffic behaviors, which will obviously have an important impact on lane changing behavior in two-lane system. However, there is always a certain deviation between the driver's optimal speed and the steady optimal speed, which has not been investigated in previous two-lane lattice models. Therefore, the optimal velocity deviation effect (OVDE) will be considered to establish a new lattice model for two lanes. Moreover, the stability condition involving the OVDE will be deduced for two lanes. Also, numerical simulations will reveal the OVDE impact on lane changing behaviors in a two-lane system according to the density evolution and hysteresis loop.

(a)E-mail: joyjc@foxmail.com (corresponding author)
(b)E-mail: guanghanpeng@163.com (corresponding author)

Modeling. – Lane changing behaviors can be seen in a two-lane system as shown in fig. 1 [47]. When $\rho_{2,j-1} > \rho_{1,j}$, there occurs an influx rate as $\gamma|\rho_0^2 V'(\rho_0)|(\rho_{2,j-1} - \rho_{1-j}))$ and when $\rho_{1,j} > \rho_{2,j+1}$, there exists an outflow rate as $\gamma|\rho_0^2 V'(\rho_0)|(\rho_{1,j} - \rho_{2,j+1}))$ at site-j on lane 1, where γ, ρ_0, and $\rho_{1,j}$ signify the rate constant coefficient, the average density and the local density at site j on lane i, respectively. Accordingly, the continuity equations were expressed as follows [47]:

$$\partial_t \rho_{1,j} + \rho_0(\rho_{1,j}v_{1,j} - \rho_{1,j-1}v_{1,j-1}) = \gamma\left|\rho_0^2 V'\right|(\rho_{2,j+1} - 2\rho_{1,j} + \rho_{2,j-1}), \tag{1}$$

$$\partial_t \rho_{2,j} + \rho_0(\rho_{2,j}v_{2,j} - \rho_{2,j-1}v_{2,j-1}) = \gamma\left|\rho_0^2 V'\right|(\rho_{1,j+1} - 2\rho_{2,j} + \rho_{1,j-1}), \tag{2}$$

where $v_{i,j}$ expresses the local velocity at site j on lane i.

Combine eqs. (1) and (2) to infer

$$\partial_t \rho_j + \rho_0\left(\rho_j v_j - \rho_{j-1}v_{j-1}\right) = \gamma\left|\rho_0^2 V'(\rho_0)\right|(\rho_{j+1} - 2\rho_j + \rho_{j-1}), \tag{3}$$

where $\rho_j = (\rho_{1,j}+\rho_{2,j})/2$ and $\rho_j v_j = (\rho_{1,j}v_{1,j}+\rho_{2,j}v_{2,j})/2$, $V' = \frac{\mathrm{d}V(\rho)}{\mathrm{d}t}\Big|_{\rho_0}$. $V(\rho)$ means the optimal velocity [47]:

$$V(\rho) = \frac{v_{\max}}{2}\left[\tanh\left(\frac{2}{\rho_0} - \frac{\rho}{\rho_0^2} - \frac{1}{\rho_c}\right) + \tanh\left(\frac{1}{\rho_c}\right)\right]. \tag{4}$$

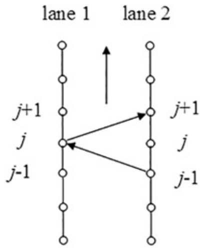

Fig. 1: The schematic for a two-lane highway.

Here ρ_c is the safety density. In addition, Nagatani [47] adopted the following flux evolution:

$$\partial_t (\rho_j v_j) = a [\rho_0 V(\rho_{j+1}) - \rho_j v_j], \tag{5}$$

where $a = 1/\tau$ is the driver's sensitivity. Also, based on Nagatani's model, some traffic factors were taken into account to build two-lane lattice models [48–59]. However, the OVDE has not been involved in previous two-lane lattice models. Consequently, a new OVDE model is described as

$$\partial_t (\rho_j v_j) = a \{\rho_0 [V(\rho_{j+1}) + \lambda (V(\rho_0) - (\rho_{j+1}))] - \rho_j v_j\}, \tag{6}$$

where $\lambda(V(\rho_0) - V(\rho_{j+1}))$ means the OVDE and λ corresponds to the response coefficient. Obviously, when $\lambda = 0$ (no OVDE), eq. (6) conforms to Nagatani's two-lane lattice model. Then, integrating eqs. (3) and (6), we get

$$\begin{aligned}&\rho_j (t + 2\tau) - \rho_j (t + \tau) + (1 - \lambda) \tau \rho_0^2 [V(\rho_{j+1}) - V(\rho_j)]\\ &-\tau\gamma \left|\rho_0^2 V'\right| [\rho_{j+1} (t + \tau) - 2\rho_j (t + \tau) + \rho_{j-1} (t + \tau)] = 0\end{aligned} \tag{7}$$

Linear stability analysis. – The density is perturbed by a small deviation y_j: $\rho_j(t) = \rho_0 + y_j(t)$. Then, eq. (7) can be transformed into the small deviation y_j via linear series expansion as follows:

$$\begin{aligned}&y_j (t + 2\tau) - y_j (t + \tau) + (1 - \lambda) \tau \rho_0^2 V' (y_{j+1} - y_j)\\ &-\tau\gamma \left|\rho_0^2 V'\right| [y_{j+1} (t + \tau) - 2y_j (t + \tau) + y_{j-1} (t + \tau)] = 0\end{aligned} \tag{8}$$

Moreover, assume $y_j = A \exp(ikj + zt)$ to get

$$\begin{aligned}&e^{2z\tau} - e^{z\tau} + (1 - \lambda) \tau \rho_0^2 V' \left(e^{ik} - 1\right)\\ &-\tau\gamma \left|\rho_0^2 V'\right| \left(e^{ik+z\tau} - 2e^{z\tau} + e^{-ik+z\tau}\right) = 0\end{aligned} \tag{9}$$

Replace $z = z_1(ik) + z_2(ik)^2 + \cdots$. Therefore, we attain the following coefficients for z_1 and z_2:

$$z_1 = (-1 + \lambda)\rho_0^2 V', \tag{10}$$

$$z_2 = \frac{1}{2}[1 + 2\gamma - \lambda + (-1 + \lambda)^2 3\rho_0^2 V'\tau]\rho_0^2 V'. \tag{11}$$

Therefore, if $z_2 < 0$, the traffic flow becomes unstable. On the contrary, if $z_2 > 0$, the traffic flow remains stable. It means that the OVDE model keeps stable in a two-lane system if

$$\tau < -\frac{1 + 2\gamma - \lambda}{(-1 + \lambda)^2\, 3\rho_0^2 V'}. \tag{12}$$

Accordingly, the neutral stability condition can be inferred as follows:

$$\tau = -\frac{1 + 2\gamma - \lambda}{(-1 + \lambda)^2\, 3\rho_0^2 V'}. \tag{13}$$

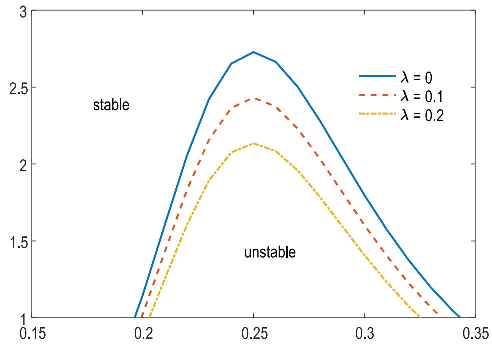

Fig. 2: Phase diagram at $\gamma = 0.05$.

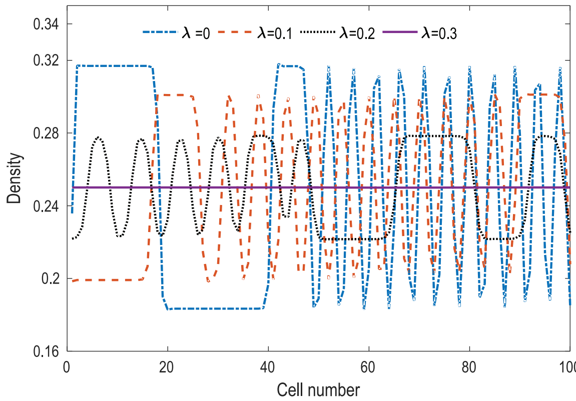

Fig. 3: The density for all cells at $t = 10300$ time step.

Figure 2 shows the stable scope according to the neutral stability curve described by eq. (13). where $v_m = 2$ and $\gamma = 0.05$. It is clear that the stable area expands with the growth of λ-value in the two-lane system from fig. 2, which demonstrates that the OVDE is beneficial to traffic stability on two lanes.

Numerical simulation. – Simulation is an important means to intuitively describe the traffic phenomenon. Then we set the initial density as

$$\begin{cases} \rho_j (0) = \rho_j (1) = \rho_0 + 0.05, & j = 50,\\ \rho_j (0) = \rho_j (1) = \rho_0 - 0.05, & j = 51,\\ \rho_j (0) = \rho_j (1) = \rho_0, & \text{other values,} \end{cases} \tag{14}$$

where $N = 100$, $\rho_0 = 0.25$, $a = 2.32$ and $\gamma = 0.05$. Also, periodic boundary is taken into account for simulation.

The density profiles in fig. 3 can be seen for all cells at time step 10300. Observed from fig. 3, the fluctuation

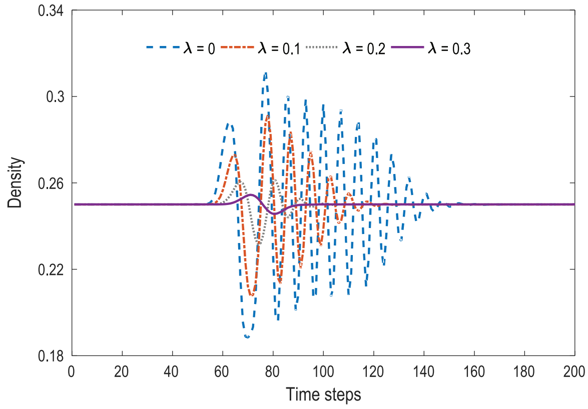

Fig. 4: The density at site 25 early time steps.

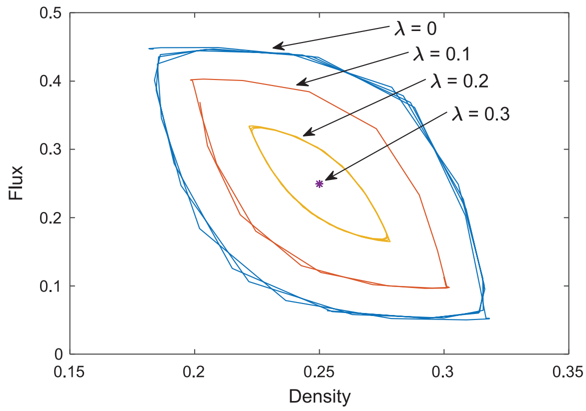

Fig. 5: The hysteresis loop at site 25.

amplitude falls down with the increase of the λ-value on the basis of density waves on two lanes. Especially, the steady density appears at $\lambda = 0.3$ on two lanes. Moreover, we observe the density evolution on site 25 at early time steps as shown in fig. 4. With the increase of λ-value, the density on site 25 tends to be stable rapidly in the early stage in two-lane system. In brief, the OVDE can maintain traffic stability well on two lanes.

Subsequently, the hysteresis loop concerning density and flux is displayed for a two-lane freeway as shown in fig. 5. The smaller the hysteresis loop area is, the smaller the fluctuation range of density and flow is. It is found that the hysteresis loop area is becoming smaller with the growth of λ-value. Finally, when $\lambda = 0.3$, the hysteresis loop condenses into one point even if lane change occurs. In short, the OVDE model contributes to alleviating the hysteresis performance.

Conclusion. – The OVDE may affect the driver's expectation of running speed. Based on this situation, we establish a new lattice model related to the OVDE for a two-lane highway. The stability condition concerning the OVDE proclaims that new consideration can ensure the stability of traffic flow on two lanes. Also, numerical simulation is implemented for the density evolution and hysteresis loop. The results tell us our model is good for improving traffic during the lane changing process on two lanes. Although our model can improve the traffic phenomena, there is a lack of calibration for some parameters. How to obtain the range of these parameters may be an interesting subject to be investigated by applying this model in the future.

* * *

This work was supported in part by the National Natural Science Foundation of China (Grant No. 61963008), Guangxi Natural Science Foundation (Grant No. 2022GXNSFDA035080), the Scientific Research Fund of Hunan Provincial Education Department, China (Grant No. 18B395).

Data availability statement: No new data were created or analysed in this study.

REFERENCES

[1] Newell G. F., *Oper. Res.*, **9** (1961) 209.
[2] Bando M., Nakayama A., Shibata A. and Sugiyama Y., *Phys. Rev. E*, **51** (1995) 1035.
[3] Nagatani T., *Phys. Rev. E*, **60** (1999) 6395.
[4] Helbing D. and Tilch B., *Phys. Rev. E*, **58** (1998) 133.
[5] Zhu W. X. and Li D. Z., *Physica A*, **492** (2018) 2154.
[6] Zhu W. X. and Zhang H. M., *Physica A*, **503** (2018) 322.
[7] Zhu W. X. and Zhang H. M., *Physica A*, **496** (2018) 274.
[8] Tang T. Q., Luo X. F., Zhang J. and Chen L., *Physica A*, **490** (2018) 1377.
[9] Tang T. Q., Rui X. X., Zhang J. and Shang H. Y., *Physica A*, **492** (2018) 1782.
[10] Tang T. Q., Yi Z. Y., Zhang J., Wang T. and Leng J. Q., *Physica A*, **496** (2018) 399.
[11] Zhang Y., Zhao M., Sun D. and Chen D., *Nonlinear Dyn.*, **103** (2021) 1891.
[12] Zeng C., Ma C. X., Wang K. and Cui Z. H., *IEEE Access*, **10** (2022) 47361.
[13] Zeng C., Ma C. X., Wang K. and Cui Z. H., *Physica A*, **599** (2022) 127498.
[14] Ma C. X., Dai Guowen G. W. and Zhou J. B., *IEEE Trans. Intell. Transp. Syst.*, **23** (2022) 5615.
[15] Ma C. X., Wang C. and Xu X. C., *IEEE Trans. Intell. Transp. Syst.*, **22** (2021) 2359.
[16] Nagatani T., *Physica A*, **261** (1998) 599.
[17] Nagatani T., *Physica A*, **264** (1999) 581.
[18] Tian J. F., Yuan Z. Z., Jia B., Li M. H. and Jiang G. J., *Physica A*, **391** (2012) 4476.
[19] Wang T., Gao Z. Y. and Zhang J., *Nonlinear Dyn.*, **73** (2013) 2197.
[20] Li Z. P., Li X. L. and Liu F. Q., *Int. J. Mod. Phys. C*, **19** (2008) 1163.
[21] Li Z. P., Liu F. Q. and Sun J., *Chin. Phys. B*, **20** (2011) 088901.
[22] Sun D. H., Tian C. and Liu W. N., *Chin. Phys. B*, **19** (2010) 080514.

[23] Tian J. F., Jia B., Li X. G. and Gao Z. Y., *Chin. Phys. B*, **19** (2010) 040303.
[24] Wang T., Gao Z. Y. and Zhao X. M., *Chin. Phys. B*, **21** (2012) 020512.
[25] Nagatani T., *Physica A*, **271** (1999) 200.
[26] Nagatani T., *Phys. Rev. E*, **59** (1999) 4857.
[27] Nagatani T., *Physica A*, **272** (1999) 592.
[28] Wang T., Gao Z. Y., Zhang J. and Zhao X. M., *Nonlinear Dyn.*, **75** (2014) 27.
[29] Li Z. P., Li W. Z., Xu S. Z. and Qian Y. Q., *Nonlinear Dyn.*, **80** (2015) 29.
[30] Gupta A. K. and Redhu P., *Commun. Nonlinear Sci. Numer. Simul.*, **19** (2014) 1600.
[31] Gupta A. K. and Redhu P., *Physica A*, **392** (2013) 5622.
[32] Gupta A. K. and Redhu P., *Nonlinear Dyn.*, **76** (2014) 1001.
[33] Gupta A. K. and Redhu P., *Phys. Lett. A*, **377** (2013) 2027.
[34] Sharma S., *Nonlinear Dyn.*, **81** (2015) 991.
[35] Redhu P. and Gupta A. K., *Nonlinear Dyn.*, **78** (2014) 957.
[36] Redhu P. and Gupta A. K., *Physica A*, **421** (2015) 249.
[37] Redhu P. and Gupta A. K., *J. Phys. A*, **445** (2016) 150.
[38] Redhu P. and Siwach V., *Physica A*, **492** (2018) 1473.
[39] Redhu P. and Gupta A. K., *Commun. Nonlinear Sci. Numer. Simul.*, **27** (2015) 263.
[40] Ge H. X., Dai S. Q., Xue Y. and Dong L. Y., *Phys. Rev. E*, **71** (2005) 066119.
[41] Ge H. X., Cheng R. J. and Lei L., *Physica A*, **389** (2010) 2825.
[42] Ge H. X., Cui Y., Zhu K. Q. and Cheng R. J., *Commun. Nonlinear Sci. Numer. Simul.*, **22** (2015) 903.
[43] Wang Y. H. X. and Ge R., *J. Phys. Lett. A*, **381** (2017) 3523.
[44] Jiang C., Cheng R. J. and Ge H. X., *Nonlinear Dyn.*, **7** (2017) 1.
[45] Wang Y., Cheng R. J. and Ge H. X., *Physica A*, **479** (2017) 478.
[46] Zhang Y. C., Zhao M., Sun D. H., Wang S. H., Huang S. and Chen D., *Commun. Nonlinear Sci. Numer. Simul.*, **94** (2021) 105541.
[47] Nagatani T., *Physica A*, **265** (1999) 297.
[48] Li Z. P., Zhang R., Xu S. Z. and Qian Y. Q., *Commun. Nonlinear Sci. Numer. Simul.*, **24** (2015) 52.
[49] Zhang G., Sun D. H. and Liu W. N., *Nonlinear Dyn.*, **81** (2015) 1623.
[50] Zhang G., Sun D. H., Liu W. N., Zhao M. and Cheng S. L., *Physica A*, **422** (2015) 16.
[51] Zhang G., Sun D. H., Zhao M., Liu W. N. and Cheng S. L., *Int. J. Mod. Phys. C*, **26** (2015) 1550062.
[52] Zhang G., Sun D. H., Liu W. N., Zhao M. and Cheng S. L., *Physica A*, **422** (2015) 16.
[53] Sharma S., *Physica A*, **421** (2015) 401.
[54] Zhu C. Q., Zhong S. Q. and Ma S. F., *Commun. Nonlinear Sci. Numer. Simul.*, **73** (2019) 229.
[55] Gong J. C., Ma C. X. and Zhu C. Q., *Mod. Phys. Lett. B*, **34** (2020) 2050250.
[56] Kaur D. and Sharma S., *Physica A*, **539** (2020) 122913.
[57] Madaan N. and Sharma S., *Physica A*, **564** (2021) 125446.
[58] Wang T., Gao Z. Y., Zhang J. and Zhao X. M., *Nonlinear Dyn.*, **75** (2014) 27.
[59] Wang T., Gao Z. Y., Zhao X. M., Tian J. F. and Zhang W. Y., *Chin. Phys. B*, **21** (2012) 070507.